# CLOUD TYPE CLASSIFICATION BY GMS-5 INFRARED SPLIT-WINDOW MEASUREMENTS WITH MILLIMETER-WAVE RADAR AND TRMM OBSERVATIONS IN THE TROPICS

Atsushi Hamada[1]*, Noriyuki Nishi[1], Hideji Kida[1], Masato Shiotani[2], Suginori Iwasaki[3], Akihide Kamei[4], Yuichi Ohno[5], Hiroshi Kuroiwa[5], Hiroshi Kumagai[5], and Hajime Okamoto[6]

1: Graduate School of Science, Kyoto University, Kyoto, Japan
2: Research Institute for Sustainable Humanosphere, Kyoto University, Kyoto, Japan
3: Institute of Observational Research for Global Change, Japan
4: National Institute for Environmental Studies, Ibaraki, Japan
5: National Institute of Information and Communications Technology, Japan
6: Graduate School of Science, Tohoku University, Sendai, Japan

## 1. INTRODUCTION

In the tropics, the upper-tropospheric cirriform clouds (UTCC), which is detrained from large-scale convective activity, often extends up to a few thousand kilometers and remains more than a day. According to numerical experiments on the life cycle of UTCC, dissipation process strongly depend on the sedimentation of cloud ice. Consequently, UTCC becomes optically thin with time and effective radiative height is lowered (*e.g.,* Boehm *et al.,* 1999).

The possible processes for maintaining or redeveloping UTCC are large-scale upward motion associated with the equatorial waves, small-scale upward motion with gravity waves, destabilization by the difference of radiative budget in UTCC, vertical diffusion, and more. However, numerical simulations concluded that these processes can maintain UTCC, but cannot redevelop UTCC (*e.g.,* Churchill and Houze, 1991).

Hamada *et al.* (2004) made the case study on the tropical large cloud disturbance, and showed that the decrease of equivalent blackbody temperature ($T_{BB}$) with time is often observed in a part of long-lasting UTCC detached from convective activity. The decrease of $T_{BB}$ implies the increase of optical thickness of UTCC due to redevelopment. The difference on the dissipation process between observation and numerical simulation is interesting issue and needs further analysis.

The analysis on the time variation of $T_{BB}$ of UTCC needs track the same cloud patch in time. Since geosynchronous satellite data have large field of view and fine time resolution, it is useful to track the cloud patches. To identify cloud types, Inoue (1987, hereafter I87) developed the cloud type classification table with split-window $T_{BB}$ (Figure 1). In this table, each observed pixel categorized into a cloud type by the two parameters, 11$\mu$m-$T_{BB}$ and the difference between 11$\mu$m-$T_{BB}$ and 12$\mu$m-$T_{BB}$. However, since this table is developed for NOAA AVHRR measurements, some modification is needed to develop this table for other satellites. Indeed, for the tracking of UTCC, the threshold for the existence of precipitation is needed, since another cumulus systems developed beneath the UTCC can also decrease $T_{BB}$.

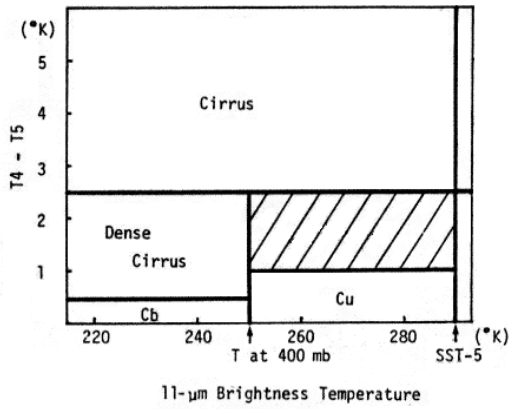


Fig. 1. Cloud type classification table developed by Inoue (1987) for NOAA AVHRR. The abscissa and ordinate shows 11 $\mu$m $T_{BB}$ and the difference between 11 $\mu$m $T_{BB}$ and 12 $\mu$m $T_{BB}$, respectively. The clear-sky region is defined as $T_{11\mu m} > SST - 5$ K. Hatched area represents non-classified region.

In this study, cloud type classification table is developed, focusing the following two points.

- Modify I87's cloud type classification table with NOAA AVHRR for GMS-5 VISSR, since these two sensors have different spectral response functions.
- Identify the threshold for the existence of precipitation, which is not shown in I87's table.

* *Corresponding author address:* Atsushi Hamada, Department of Geophysics, Graduate School of Science, Kyoto University, Kyoto 606-8502, Japan; e-mail: hamada@kugi.kyoto-u.ac.jp

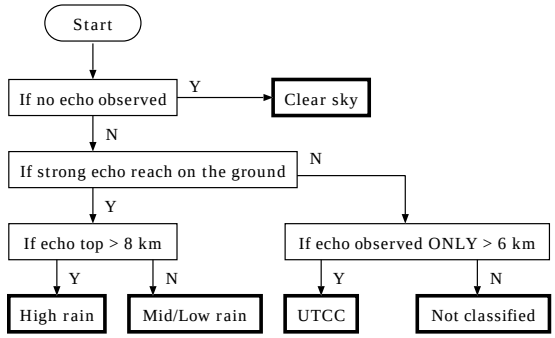


Fig. 2. Flow chart for the cloud type classification by millimeter-wave radar echo.

To identify cloud type by ground-base observation, millimeter-wave cloud radar is used in this study. Millimeter-wave cloud radar has great advantage for observation of the vertical structure of geometrical or optical thick non-precipitating ice clouds, which is hard to be observed by precipitation radar and lidar.

## 2. DATA

To make the cloud type classification table, we use the millimeter-wave cloud radar (SPIDER) data and GMS-5 infrared $T_{BB}$ data. The SPIDER is 95-GHz airborne cloud profiling radar with 82.5-m range resolution. We use the data during the period from 9 November to 9 December 2001, when the SPIDER was fixed at the research vessel Mirai and made vertical observations around (138°E, 2°N). GMS-5 data provides hourly 11-$\mu$m and 12-$\mu$m infrared $T_{BB}$, with 0.05° resolution.

To validate the classification table, we also use TRMM Microwave Imager (TMI) 2A12 surface rain data.

## 3. CLOUD TYPE CLASSIFICATION

Figure 2 shows the flow chart for cloud type classification. In this study, the vertical profiles of millimeter-radar echo averaged over 5 minutes are categorized into five types.

When no echo is observed vertically, the echo profile is identified as clear-sky. If the strong echo reaches on the ground, the profile is identified as precipitating cloud. Precipitating clouds are further categorized by the echo top height. Echo top height in this case is defined as the height where reflectivity factor first reaches noise level. Clouds with echo top higher than 8 km is categorized into high precipitating clouds, and clouds with echo top lower than 8 km is categorized into middle/low ones. High and middle/low precipitating clouds implies cumulonimbus and cumulus congestus or shallow cumulus, respectively (Johnson *et al.,* 1999). Note that middle/low precipitating clouds may include the multi-layered clouds such as cumulus overlapped by high cirrus. For clouds without precipitation, the clouds with echo bottom higher than 6 km is identified as upper-tropospheric cirriform clouds. Other echo profiles are out of classification in this study. Such clouds include liquid or mixed phase clouds in the middle troposphere.

To estimate the optical thickness of the non-precipitating cirriform cloud, at first the reflectivity $Z_e$ is converted into ice water content (IWC) by the following equation suggested by Liu and Illingworth (2000):

$$\mathrm{IWC} = 0.137 {Z_e}^{0.643}.$$

Next, cloud ice water path (IWP) is calculated by integrating IWC from the bottom to the top of the cloud. Finally, optical depth in visible wavelengths is estimated by the following relationship based on observations (Heymsfield *et al.,* 2003):

$$\tau_{\mathrm{vis}} = 0.065 \mathrm{IWP}^{0.84}.$$

## 4. RESULTS

During the analysis period, there was 783 radar echo profiles in which the difference of observation time is within 1 minute between GMS-5 and SPIDER. For each profile, the cloud type is identified. Corresponding $T_{BB}$ is calculated as the average over four pixels including the observation point.

Figure 3 shows the scatter plot of cloud types. Broken lines show the thresholds for cloud type classification by I87.

In the area with low $T_{11\mu m}$, most of precipitating clouds have the value $T_{11\mu m} - T_{12\mu m}$ less than 1.8 K. This fact shows that we can use the value $T_{11\mu m} - T_{12\mu m} = 1.8$ K as the threshold for the existence of precipitation. It should be noted that some non-precipitating cirriform clouds also have the value $T_{11\mu m} - T_{12\mu m} < 1.8$ K.

Comparing with I87, clouds which are classified as dense cirrus by I87 include many precipitating clouds. The threshold $T_{11\mu m} - T_{12\mu m} = 0.5$ K used in I87's table implies the threshold between convective and stratiform precipitation in the table developed in this study, but further analysis is needed.

For the non-precipitating UTCC, clouds with larger optical thickness have lower $T_{11\mu m}$. Note

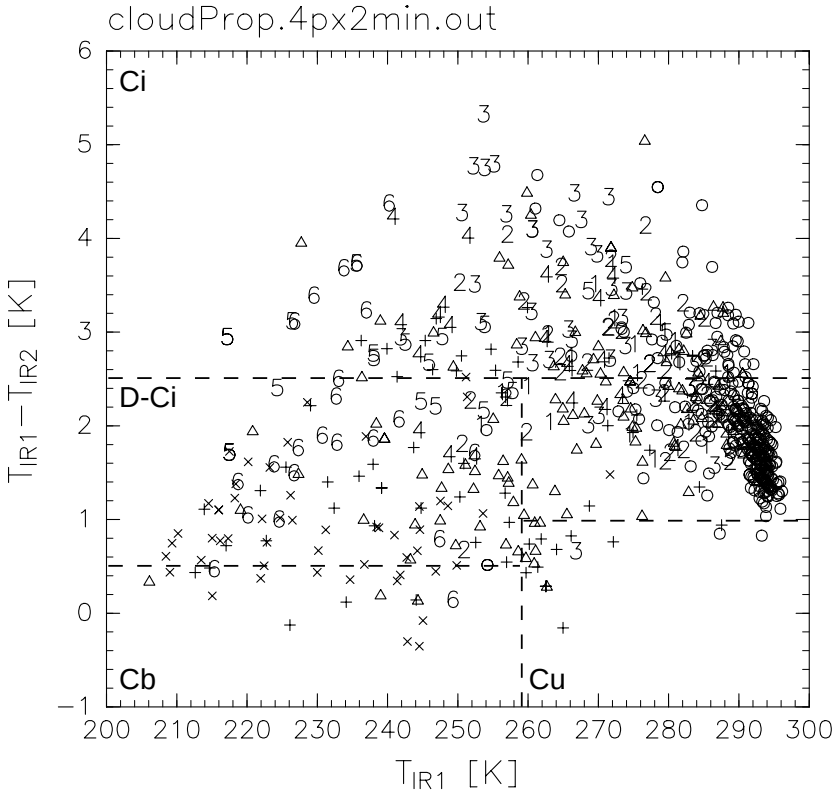


Fig. 3. Scatter plot of cloud types classified by millimeter-wave radar. The abscissa and ordinate shows $T_{11\mu m}$ and the difference between $T_{11\mu m}$ and $T_{12\mu m}$, respectively. The label $\times$ represents high precipitating clouds, + middle/low precipitating clouds, $\circ$ clear-sky, and $\triangle$ non-classified clouds. Numbers (1-6) represents non-precipitating UTCC and larger number shows optically thicker UTCC. Broken lines show the thresholds for the classification by I87, where Cb is classified as cumulonimbus, D-Ci as dense cirrus, Ci as thin cirrus, Cu as cumulus.

that, while in I87 optically thick and thin cirrus is classified in lower and upper side of the line $T_{11\mu m} - T_{12\mu m} = 2.5$ K, respectively, in Fig. 3 optical thickness of UTCC is related with rather $T_{11\mu m}$ than $T_{11\mu m} - T_{12\mu m}$. Figure 4 shows the histogram of non-precipitating thick ($\tau_{vis} > .5$) and thin ($\tau_{vis} < .5$) UTCC in each 10 K bin of $T_{11\mu m}$. In this study, we choose $T_{11\mu m} = 250$ K as the threshold between thick and thin UTCC.

## 5. VALIDATION WITH TRMM

The cloud type classification table suggested in this study, is validated with rain observation by TRMM. Figure 5 shows GMS-5 $T_{BB}$ and TMI surface rain at the almost same time. The area classified as high-precipitating clouds is indicated by contours superposed on the surface rain field. Classified area encompasses the whole area with heavy rain, while the area with no rain is partly included.

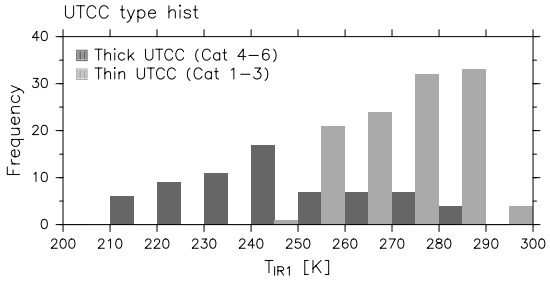


Fig. 4. Histogram of non-precipitating thick ($\tau_{vis} > .5$) and thin ($\tau_{vis} < .5$) UTCC in each 10 K bin of $T_{11\mu m}$.

## 6. DISCUSSION

### 6.1 *Middle/low precipitating clouds overlapped by high ice clouds*

Figure 6 shows the example of the clouds classified as middle/low precipitating clouds by cloud radar, which located around $230 < T_{11\mu m} < 260$ K and $2.5 < T_{11\mu m} - T_{12\mu m} < 3.2$ K in Fig. 3. These

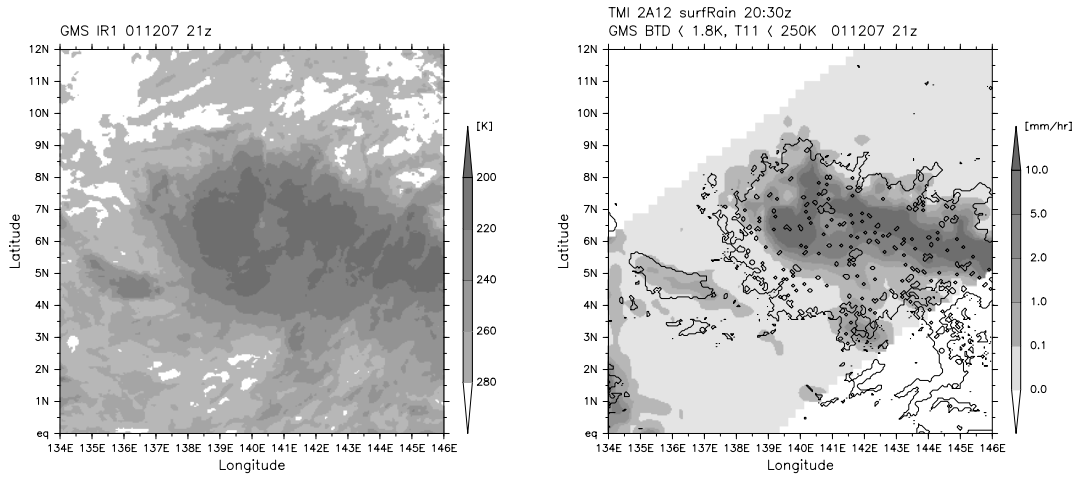


Fig. 5. (Left) GMS-5 $T_{BB}$ at 21 UTC 7 December 2001. (Right) TMI 2A12 surface rain (grayscale) and the area classified as high-precipitating cloud (solid contours)

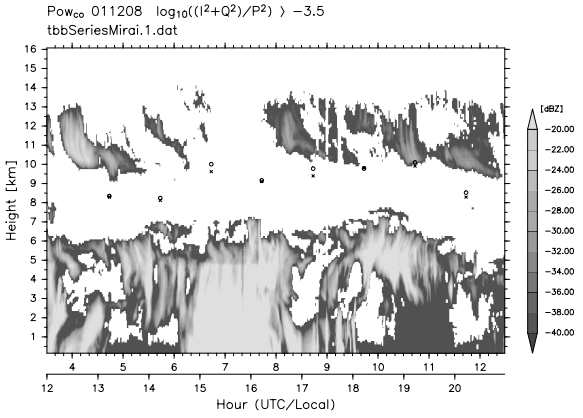


Fig. 6. Time-height cross section of cloud radar reflectivity factor $dBZ_e$, from 03:30 UTC 8 December 2001. Corresponding local time at R/V Mirai is also shown. The labels $\times$ and $\circ$ represents the converted heights of $T_{11\mu m}$, $T_{12\mu m}$ estimated by and climatological vertical profile of temperature, respectively.

clouds are multi-layered where middle precipitating clouds are covered by high non-precipitating cirriform clouds. It is implied that overlapped high ice clouds increase the value $T_{11\mu m} - T_{12\mu m}$, further analysis is needed about the frequency of occurrence of such multi-layered clouds in the Tropics, and radiative characteristics in the split-window wavelengths.

## 7. CONCLUSIONS

Cloud type classification table with GMS-5 split-window $T_{BB}$ is developed. Millimeter-wave cloud radar is used to identify each cloud type. In this table, pixels observed by GMS-5 are categorized into five types by the two parameter, $T_{11\mu m}$ and the difference between $T_{11\mu m}$ and $T_{12\mu m}$.

For clouds with low $T_{11\mu m}$, the existence of precipitation is identified as $T_{11\mu m} - T_{12\mu m} = 1.8$ K, if clouds are not multi-layered. Note that the area $T_{11\mu m} - T_{12\mu m} < 1.8$ K includes some non-precipitating cirriform clouds. Non-precipitating UTCC is classified as thick ($\tau_{vis} > .5$) and thin ($\tau_{vis} < .5$) with the threshold $T_{11\mu m} = 250$ K.

### References


Boehm, M. T., J. Verlinde, and T. P. Ackerman, 1999: On the maintenance of high tropical cirrus. *J. Geophys. Res.,* **104,** 24423-24433.

Churchill, D. D., and R. A. Houze, Jr., 1991: Effects of radiation and turbulence on the diabatic heating and water budget of the stratiform region of a tropical cloud cluster. *J. Atmos. Sci.,* **48,** 903-922.

Hamada, A., N. Nishi, and H. Kida, 2004: Deformation of large cloud disturbance over the western tropical Pacific. in revision.

Heymsfield, A. J., S. Matrosov, and B. Baum, 2003: Ice water path-optical depth relationships for cirrus and deep stratiform ice cloud layers. *J. Appl. Meteor.,* **42,** 1369-1390.

Inoue, T., 1987: A cloud type classification with NOAA 7 split-window measurements. *J. Geophys. Res.,* **92,** 3991-4000.

Johnson, R. H., T. M. Rickenbach, S. A. Rutledge, P. E. Ciesielski, and W. H. Shubert, 1999: Trimodal characteristics of tropical convection. *J. Climate,* **12,** 2397-2418.

Liu, C.-L., and A. J. Illingworth, 2000: Toward more accurate retrievals of ice water content from radar measurements of clouds. *J. Appl. Meteor.,* **39,** 1130-1146.